

NATIONAL AERONAUTICS AND SPACE ADMINISTRATION

Technical Report 32-1220

Lunar Orbiter Data Analysis

J. Lorell
W. L. Sjogren

GPO PRICE \$ _____

CFSTI PRICE(S) \$ _____

Hard Copy (HC) _____

Microfiche (MF) _____

ff 653 July 65

FACILITY FORM 602

N 68-12908
(ACCESSION NUMBER)

18
(PAGES)

CR-91374
(NASA CR OR TMX OR AD NUMBER)

(THRU)

30
(CODE)

(CATEGORY)

JET PROPULSION LABORATORY
CALIFORNIA INSTITUTE OF TECHNOLOGY
PASADENA, CALIFORNIA

November 15, 1967

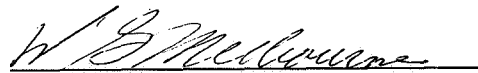
NATIONAL AERONAUTICS AND SPACE ADMINISTRATION

Technical Report 32-1220

Lunar Orbiter Data Analysis

*J. Lorell
W. L. Sjogren*

Approved by:

A handwritten signature in dark ink, appearing to read "W. G. Melbourne", is written over a horizontal line.

W. G. Melbourne, Manager
Systems Analysis Research Section

JET PROPULSION LABORATORY
CALIFORNIA INSTITUTE OF TECHNOLOGY
PASADENA, CALIFORNIA

November 15, 1967

TECHNICAL REPORT 32-1220

Copyright © 1967
Jet Propulsion Laboratory
California Institute of Technology

Prepared Under Contract No. NAS 7-100
National Aeronautics & Space Administration

Contents

I. Introduction	1
II. Discussion	1
A. Temperature Effect Due to Spacecraft-Sun Occultation	2
B. Attitude Control Forces of the Spacecraft.	2
C. Atmospheric Drag	4
D. Ionosphere	4
E. Doppler Theoretical Calculation by Range Differencing	5
F. Integrated Doppler Compared to Range Data	5
G. Single-Precision Versus Double-Precision Integration	5
H. Langley Research Center Comparison	6
I. Tracking Station Bandwidth	6
J. Multipath	6
K. Least-Squares Filter Effect	6
L. Residuals In-Plane Versus Out-Of-Plane	7
M. Modified Potential Models	7
N. Frequency Analysis on Residuals	8
O. Lunar Ephemeris Position and Velocity Errors Model	10
P. Frequency Bias on Three-Way Doppler	11
Q. Radiation Pressure	11
III. Conclusions	11
References	12

Table

1. Perturbations caused by lunar ephemeris errors	12
---	----

Figures

1. <i>Lunar Orbiter IV</i> doppler residuals—Goldstone, June 17, 1967 (22 h 50 min)	2
2. <i>Lunar Orbiter IV</i> doppler residuals—Goldstone, June 7, 1967 (14 h 56 min)	2

Contents (contd)

Figures (contd)

3. <i>Lunar Orbiter IV</i> limit cycle control, June 10, 1967 (limit cycle = 0.2 deg)	3
4. <i>Lunar Orbiter IV</i> limit cycle control (limit cycle = 2 deg)	4
5. Changes in semimajor axes, <i>Lunar Orbiters I</i> and <i>II</i>	4
6. Geometry of possible ionosphere about the moon	4
7. Mark I-A ranging residual of <i>Lunar Orbiter IV</i>	5
8. Difference in geocentric range rate from single- and double-precision integrations	6
9. Averaged eccentricity, <i>Lunar Orbiter I</i>	6
10. DSS 12 residuals, Aug. 26, 1966 (5 h 20 min)	7
11. In-plane vs out-of-plane doppler residuals	7
12. DSS 12 residuals, Aug. 26, 1966 (5 h 19 min)	8
13. DSS 12 residuals, Nov. 22, 1966 (5 h 17 min)	8
14. DSS 41 residuals, Nov. 22, 1966 (5 h 18 min)	8
15. DSS 41 residuals, Aug. 28, 1966 (12 h 45 min)	8
16. Doppler residuals, Aug. 28, 1966 (lunar coefficients = 0)	9
17. Energy density, Aug. 26, 1966 (5 h 19 min)	9
18. Energy density, DSS 12, Nov. 22, 1966 (5 h 17 min)	9
19. Energy density, DSS 41, Nov. 22, 1966 (5 h 17 min)	10
20. Energy density, Aug. 28, 1966 (12 h 45 min)	10
21. Energy density, Aug. 28, 1966 (12 h 45 min), lunar coefficients = 0	11
22. DSS 41 doppler residuals on bias fit, Aug. 26, 1966 (8 h 20 min)	11

Abstract

Lunar Orbiter tracking data have been consistently characterized by large doppler residuals near pericyynthion. Attempts to explain this phenomenon have led to an intensive investigation of possible causes, covering numerical procedures, instrument operation, and physical model. This report documents the investigation and interprets the results.

Lunar Orbiter Data Analysis

I. Introduction

During the past year, tracking data from five *lunar orbiters* have been received and processed successfully for project operations. However, attempts to process these data for scientific applications have brought on doubts as to the validity of the data, the accuracy of the theoretical model, the completeness of the model, and the behavior of the spacecraft. Many tests have been conducted in these areas and this report is intended to document these tests, so that they can be reviewed and will not have to be re-evaluated in the future. The high amplitude oscillation of the doppler residuals when the spacecraft is at closest approach to the lunar surface is the primary anomalous effect noted.¹ These oscillations are from 1 to 10 Hz² on a least-squares fit, whereas, on translunar trajectories, the residuals are on the order of 0.005 Hz. All *lunar orbiters* exhibit this characteristic although the amplitude is not as large for the orbits with higher closest-approach altitudes.

II. Discussion

The items listed below and briefly discussed in the following subsections have been considered as possible

pertinent factors in explaining the closest-approach residuals:

- (1) Temperature effect due to spacecraft-sun occultation.
- (2) Attitude control forces of the spacecraft.
- (3) Atmospheric drag.
- (4) Ionosphere.
- (5) Doppler theoretical calculation by range differencing.
- (6) Integrated doppler compared to range data.
- (7) Single-precision versus double-precision integration.
- (8) Langley Research Center comparison.
- (9) Tracking station bandwidth.
- (10) Multipath.
- (11) Least-squares filter effect.
- (12) Residuals in-plane versus out-of-plane.
- (13) Modified potential models.
- (14) Frequency analysis on residuals.
- (15) Lunar ephemeris position and velocity errors.

¹Sometimes referred to as perilune or perifocus.

²1 Hz = 65 mm/s.

(16) Frequency bias on three-way doppler.

(17) Radiation pressure.

A. Temperature Effect Due to Spacecraft-Sun Occultation

Temperature effect was one of the first suggested possible causes of the characteristic residuals at perilune (Fig. 1). However, since the mission was designed for good lighting conditions at closest approach, sun occultation and closest approach were occurring at approximately the same time at the beginning of each mission. It was not until a mission had progressed for several months and these two parameters had changed relatively, that temperature effect could be determined as negligible. *Lunar Orbiter IV*, whose orbit was continuously in the sunlight and the oscillations in the residuals still occurred at closest approach (Fig. 2), provided additional evidence that temperature effect was not the cause of residuals.

B. Attitude Control Forces of the Spacecraft

Attitude control forces are produced by three sets of gas jets that keep the spacecraft inertially positioned in

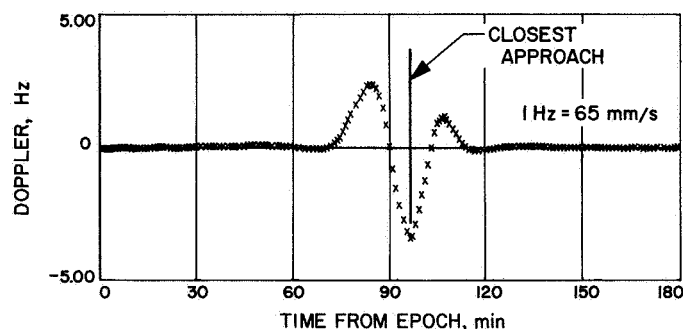


Fig. 1. *Lunar Orbiter IV* doppler residuals—Goldstone, June 17, 1967 (22 h 50 min)

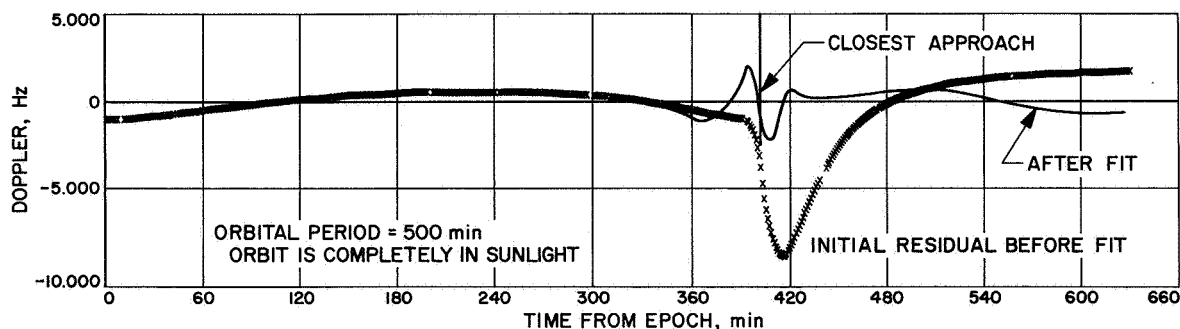


Fig. 2. *Lunar Orbiter IV* doppler residuals—Goldstone, June 7, 1967 (14 h 56 min)

pitch, roll, and yaw, respectively. Ideally, each set should produce a perfect couple which would not apply any translational force to the spacecraft when it is overcoming solar pressure and gravity gradient torques. However, on the *Lunar Orbiters*, only the roll jets are coupled. Because the pitch and yaw jets are not coupled, a side force is produced whenever these jets are used. Although these jets are used quite often, the sum total impulse is small. An actual record of their use is shown in Figs. 3 and 4. It should be noted that the period of the limit cycle was changed from 0.2 deg, as shown in Fig. 3, to 2 deg prior to the data used for Fig. 4. Over a one-orbit period, the total doppler contribution was approximately 0.01 Hz, determined as follows:

$$a = \frac{F}{M}$$

where

$$F = 0.05 \text{ lb force from a pitch jet}$$

$$M = \frac{635}{32.2} = 19.7 \text{ slugs}$$

$$a = 0.05/19.7$$

$$= 0.00254 \text{ ft/s}^2$$

$$= 0.0116 \text{ Hz/s}$$

If it is assumed that the jet always fires in the same direction (the worst case) and for 20 ms (conservative since firing duration varies from 11 to 20 ms) 40 times in one orbit, the net velocity change, ΔV , would be

$$\Delta V = 0.0116 (40) (0.02) = 0.0093 \text{ Hz}$$

These side forces, however, are much too small to explain the doppler residuals observed at perilune.

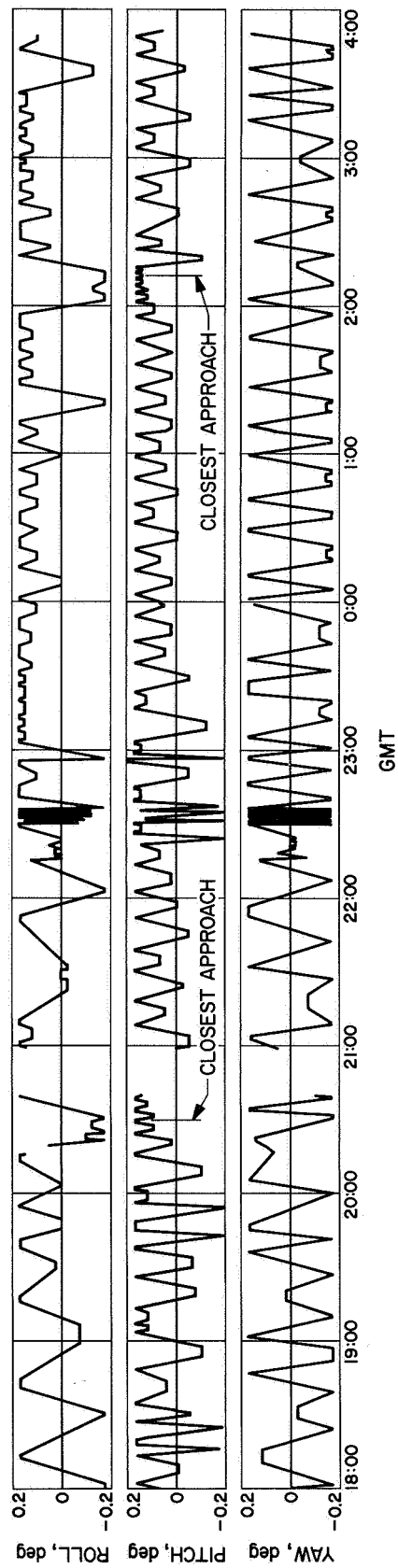


Fig. 3. Lunar Orbiter IV limit cycle control, June 10, 1967 (limit cycle = 0.2 deg)

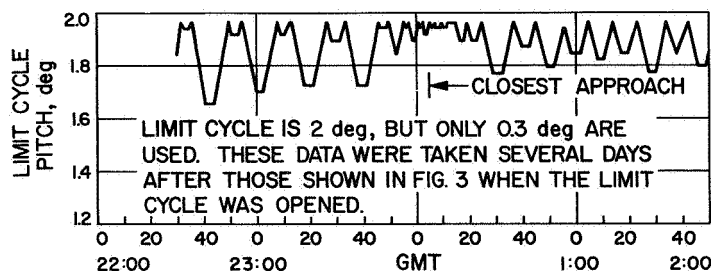


Fig. 4. Lunar Orbiter IV limit cycle control (limit cycle = 2 deg)

Finally, it should be noted that the pitch-jet side force is somewhat smaller, although of the same order of magnitude as the solar pressure force. For example, the computed acceleration due to solar pressure is approximately $1.1 \times 10^{-7} \text{ m/s}^2$, while the pitch-jet force computed above amounts to $0.04 \times 10^{-7} \text{ m/s}^2$.

C. Atmospheric Drag

An atmosphere on the moon would produce drag on the spacecraft and cause the semimajor axis of the spacecraft orbit to decay in time. Data are now available on three orbiters for periods of several months and, in all cases, the average semimajor axis over one orbit is constant within the precision of the measurements. The measurements might possibly be interpreted as a positive drift of approximately 200 m per month (Fig. 5). However, this is an increase in energy that could not be attributed to drag, because drag decreases the energy of the spacecraft.

To produce an effect measurable by doppler in one orbit, the velocity would have to be changed by at least 0.05 Hz ($= 0.003 \text{ m/s}$), which corresponds to 17.5 m per orbit or a change of semimajor axis of 120 m per day. Figure 5 shows that there is no such effect. Therefore, it can be concluded that drag effects are not detectable over one orbit, and they certainly could not produce the 5-Hz doppler residuals observed near perilune.

D. Ionosphere

The possible existence of an ionosphere about the moon that would cause the perilune residuals was considered. However, when the geometry was studied, the predominant area of largest ionospheric effect was not correlated with the closest approach point where the residuals were predominantly so much larger.

The geometry illustrated in Fig. 6 shows that an observer on the earth views the satellite at point A on the

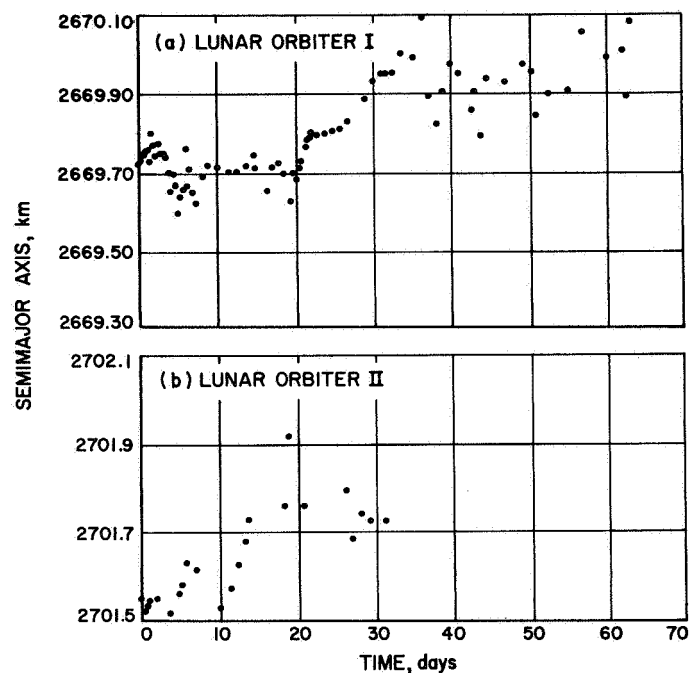


Fig. 5. Changes in semimajor axes, Lunar Orbiters I and II

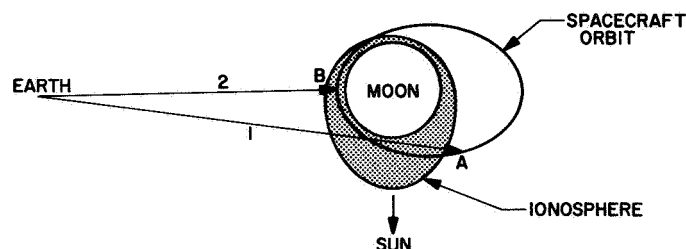


Fig. 6. Geometry of possible ionosphere about the moon

orbit along ray 1, which passes through much more of any ionosphere the moon may have, than does ray 2 to point B.

If the signal were changed at all by the ionosphere, it would be changed more along ray 1 than ray 2. However, in the data residuals, nothing of significance is seen at point A, thus corroborating the lack of an appreciable ionosphere.

E. Doppler Theoretical Calculation by Range Differencing

It has been suggested that the computation of doppler frequency in the Orbit Determination Program (ODP) may be in error or inaccurate enough to contribute to the perilune residual problem. However, a simple check on the computations has demonstrated that this is not the case.

The basic observable in doppler tracking is the frequency, f , defined with respect to a count time τ as the total number of cycles $N(\tau)$ received during the time interval τ divided by τ

$$f = \frac{1}{\tau} N(\tau)$$

Because the wavelength of the radar signal is known, $N(\tau)$, which corresponds to the change in path length of the signal during interval τ , can be computed. Therefore, to obtain the computed value of the observable f , it is more realistic to compute the path lengths at the beginning and at the end of the interval, subtract, and divide by τ .

Unfortunately, this procedure involves the differencing of nearly equal large numbers, resulting in a loss of precision. The ODP avoids this problem by using an alternate computation procedure which depends on Taylor series expansions of the frequency. The formulas are considerably more complicated than those of the range-differencing method, and give rise to questions of rate of series convergence, truncation error, coding errors, and perhaps other numerical problems.

The procedure in the ODP was checked directly by range differencing to determine the adequacy of the computation. This approach was not used before because it lacked precision in computing the station range using the single precision program with 8% bits per word. Recently, the double-precision program became available, and these computations were carried out. Two specific points with large doppler residuals (5 Hz) were chosen and the comparison between the doppler calculated in the usual manner, and that calculated with range

differencing, showed agreement to 0.02 Hz. This difference is too small to explain the doppler residuals at perilune.

F. Integrated Doppler Compared to Range Data

The accuracy of the doppler computation also can be checked by comparing the range data to the integrated doppler. In Ref. 2, Liu shows that the doppler data are essentially the same as the differenced range data. Liu processes the raw data from both doppler and range by simply differencing two range points and comparing the result with the accumulated doppler cycle count over the same time span. Figure 7 shows how well these data agree. Liu is primarily looking for ionospheric effects near the earth by differencing these two data types. These data types should show a small difference because doppler travels at a phase velocity, and ranging travels at a group velocity. This slowly varying ionospheric effect of 10 m in 6 h produces approximately a 0.005-Hz doppler residual. Therefore, the two independent data types are displaying the same characteristics in the data, for if the oscillations were not in the range data, there would be differences of 100 m rather than only a few meters.

G. Single-Precision Versus Double-Precision Integration

The precision of the integrating package in the single-precision program has been checked by comparison with

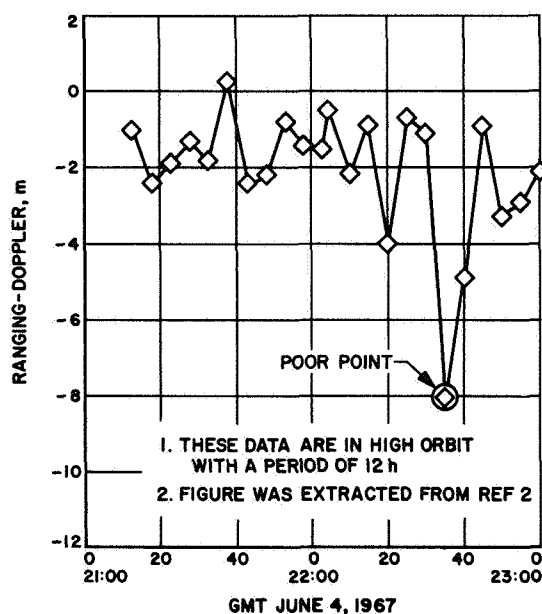


Fig. 7. Mark I-A ranging residual of Lunar Orbiter IV

the double-precision program. The comparison reveals that the selenocentric positions and velocities after one orbit of computation differ by 0.5 m and 0.003 m/s, respectively, and that the geocentric range rates (doppler) differ by 0.003 m/s (Fig. 8). These effects are much too small to contribute noticeably to the perilune residuals.

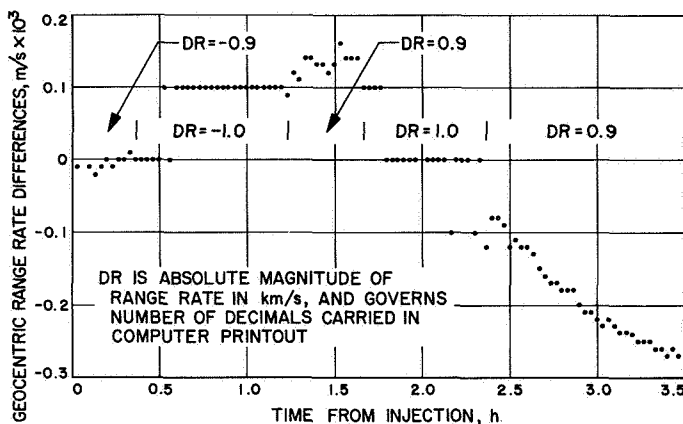


Fig. 8. Difference in geocentric range rate from single- and double-precision integrations

H. Langley Research Center Comparison

An independent double-precision computer program was developed at Langley Research Center. The program produces the same characteristic residuals near the closest approach point. Even long-term estimates of orbital elements are the same as those obtained in the present program at JPL. The data in Fig. 9 agree with Langley's results within the accuracy of the computations. Again, this confirms that the computations in the program are being performed as specified.

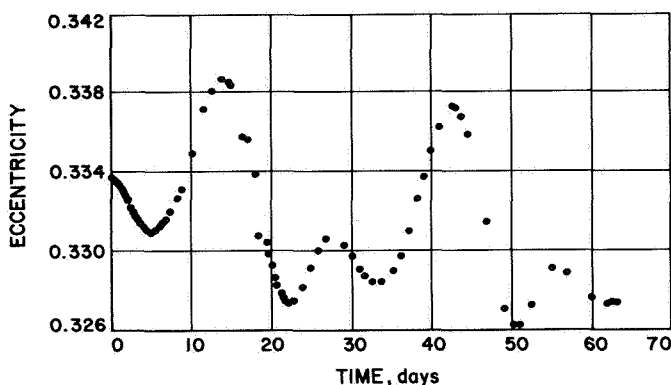


Fig. 9. Averaged eccentricity, Lunar Orbiter I

I. Tracking Station Bandwidth

The setting of the tracking station receiver bandwidth was checked for its effect on the residuals. The station tracked one orbit with the setting wide open³ and the next orbit with a setting as narrow as possible. It was thought the narrow setting would possibly corrupt the data because it had to pass through more filters. The residuals agreed to less than 0.02 Hz, showing that the station receiver bandwidth had no effect. If the signal strength would have been low, the station receiver bandwidth might have had an effect; however, power has been adequate on all orbiters.

J. Multipath

Multipath is the effect of having a reflected signal (spacecraft-moon-earth instead of spacecraft-earth) counted with the normal signal. The strength of such a signal should be low and never picked up once the main signal is obtained. However, it has been suggested that there might be a small, but detectable, multipath effect when the line of sight to the spacecraft is nearly perpendicular to the lunar surface.

The orbits of *Lunar Orbiters IV* and *V* provided tracking opportunities when the line of sight to the spacecraft never intersected the moon, therefore minimizing the possibility of multipath effects. Because the oscillations of the closest approach residuals were observed in these instances, multipath has been ruled out as the source of residuals.

K. Least-Squares Filter Effect

The least-squares fitting procedure can sometimes yield misleading results when an incomplete or erroneous model is used. If, for example, an important parameter is omitted from the model, the contributions of this parameter to the residuals may be absorbed by other parameters with which it is partly correlated. The following example using simulated data for *Lunar Orbiter I* demonstrates this effect.

A simulated data tape using the value $J_{20} = 2 \times 10^{-4}$ was generated. The value for J_{20} was set to zero and the least-squares routine, which estimated the position and velocity of the spacecraft, fitted the data as well as possible. The residuals for $J_{20} = 0$ were 21 Hz initially, but, after the fit, the residuals were approximately 1 Hz. Figure 10 shows these residuals (note scales). This points

³Bandwidth settings: wide, 500 Hz; narrow, 120 Hz (not threshold, but at -100 dBmW).

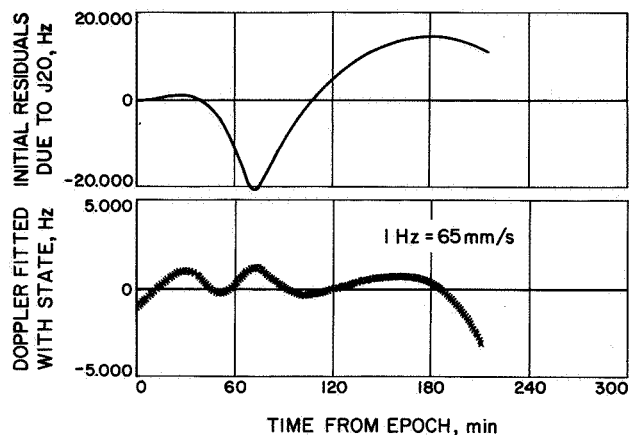


Fig. 10. DSS 12 residuals, Aug. 26, 1966
(5 h 20 min)

out that, although the fitted real data have residuals of 1 to 10 Hz, in reality there may be residuals of 100 Hz caused by some unmodeled parameter that is being least-squares fitted with an incomplete estimation set.

L. Residuals In-Plane Versus Out-Of-Plane

With *Lunar Orbiter IV*⁴ there were times when the geometry of the orbit was such that the line of sight from the earth was normal to the spacecraft orbit plane and, seven days later, the line of sight was essentially in the orbit plane. It was then possible to observe the amplitude of the residuals out-of-plane and in-plane. If the

⁴Inclination to the lunar equator plane 85 deg.

residuals were the same for both situations, then a stronger case might be built for assuming that the signal is being corrupted by a medium that it must pass through. However, if the out-of-plane residuals were smaller (factor of approximately 3) than the in-plane residuals, then the case for lunar potential harmonics would be strengthened.⁵ Figure 11 displays the residuals obtained when data in-plane and out-of-plane respectively are fit using a potential model consisting of nominal values on J20 and C22 and all other coefficients set to zero. Only the spacecraft's position and velocity were estimated. The residuals from the in-plane fit are much larger than those from the out-of-plane fit and, therefore, add to the evidence that these anomalies at pericenter are caused by the lunar potential.

M. Modified Potential Models

A modified computer program capable of adding a small term to the lunar potential was developed to determine whether a simpler model could handle the residuals. The term added to the primary acceleration term ($-GM/R^2$) was $K/|\mathbf{R} - c\mathbf{r}_e|^2$, where K and c are constants and \mathbf{r}_e is a unit vector on the earth-moon line and \mathbf{R} is the radius vector to the satellite. The constants K and c were chosen to minimize the sums of the square of the residuals. However, no appreciable improvement in the fit to the data was obtained, and the attack was

⁵Comment by W. M. Kaula that experience on earth orbiters gave as a rule of thumb a 3- to 4-time larger effect on in-plane data than on out-of-plane.

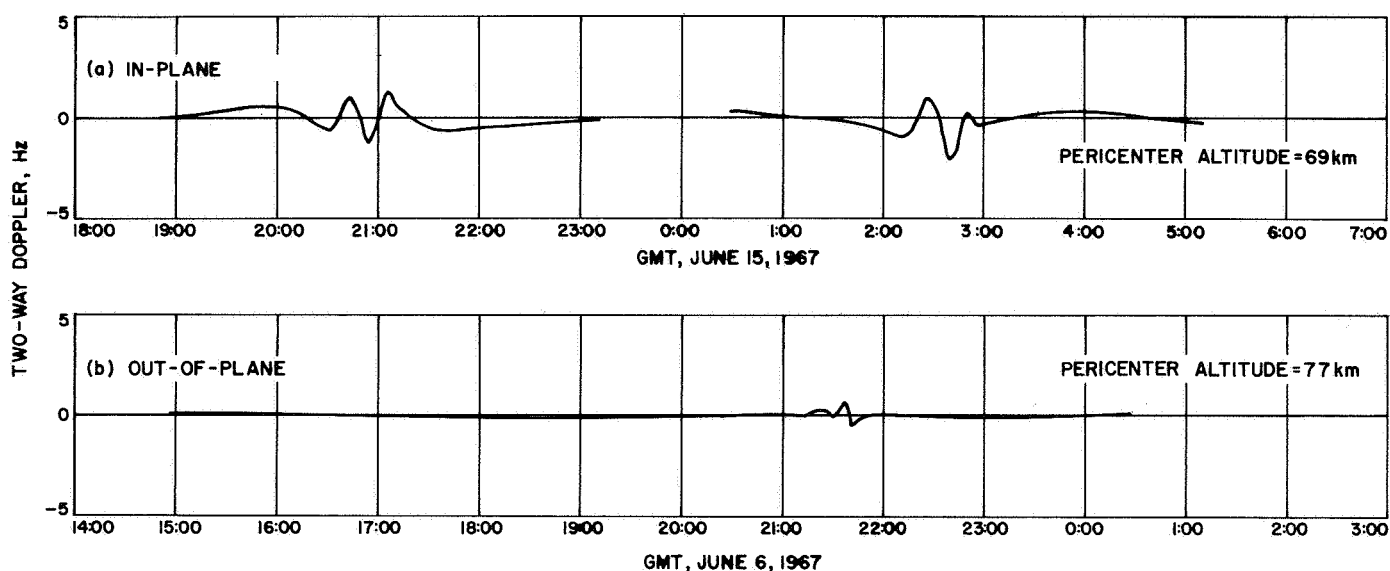


Fig. 11. In-plane vs out-of-plane doppler residuals

abandoned. At present a slightly different term has been added to the acceleration, $K/(R - C)^P$, where K , C , and P are input constants, and there is no dependence on the earth-moon line. Initially, C was chosen as the lunar radius to emphasize altitude dependence. Results showed no significant improvement in the fit and the solutions obtained for K were small.

N. Frequency Analysis on Residuals

Because the highest degree harmonic coefficients (degree and order 4) used in the estimation process did not account for the oscillations in the residuals, it was decided to determine what frequencies remained in the residuals after the fit, and possibly obtain a bound on the degree of the harmonics that should be estimated for removal of these residuals.

Because this potential model expresses accelerations as functions of sines and cosines of selenographic latitude and longitude, several assumptions for correlation and simplification were made. The inclination of the spacecraft orbit to the lunar equator being 12 deg, the latitude of the orbit was never greater than this. Therefore, it was assumed that the latitude effect was secondary. To accommodate the longitude effect, the doppler data, which were originally produced as a function of time, were converted to a function of true anomaly which varies approximately as the longitude. The doppler data, thus expressed, should exhibit the same frequencies as the potential model. Then, with a frequency analysis computer program based on Fourier transformations, the doppler data residuals over one orbit (actually only 0.8 of an orbit since there was a period of occultation) were

processed. It was hoped that some frequencies (cycles/spacecraft orbit) would stand out significantly above the others, and that consideration could then be given to including at least these frequencies in the potential model and for estimation in the orbit determination program.

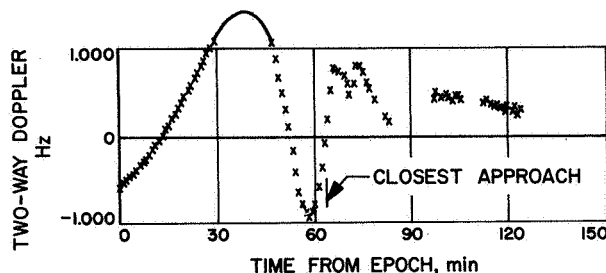


Fig. 13. DSS 12 residuals, Nov. 22, 1966
(5 h 17 min)

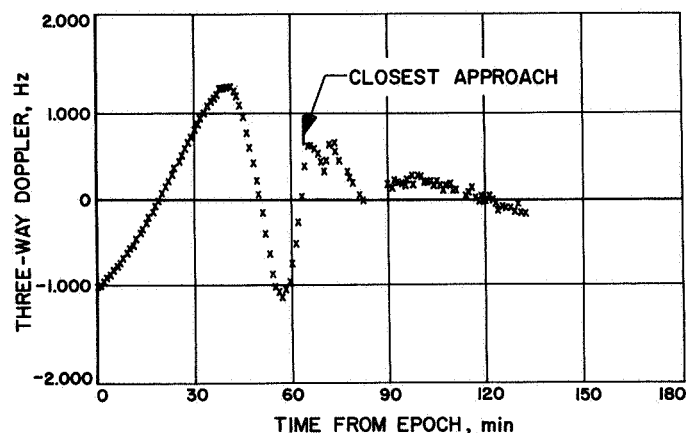


Fig. 14. DSS 41 residuals, Nov. 22, 1966
(5 h 18 min)

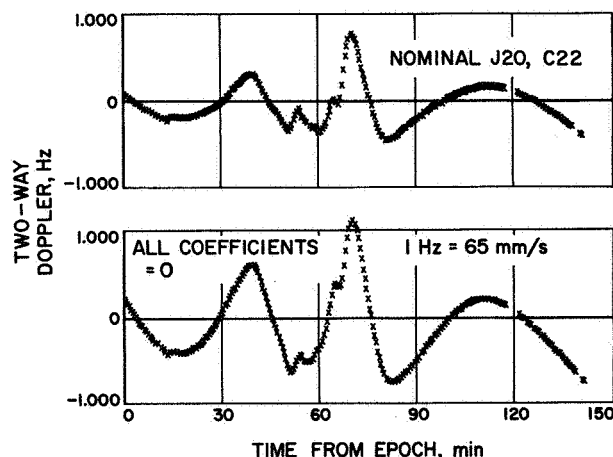


Fig. 12. DSS 12 residuals, Aug. 26, 1966
(5 h 19 min)

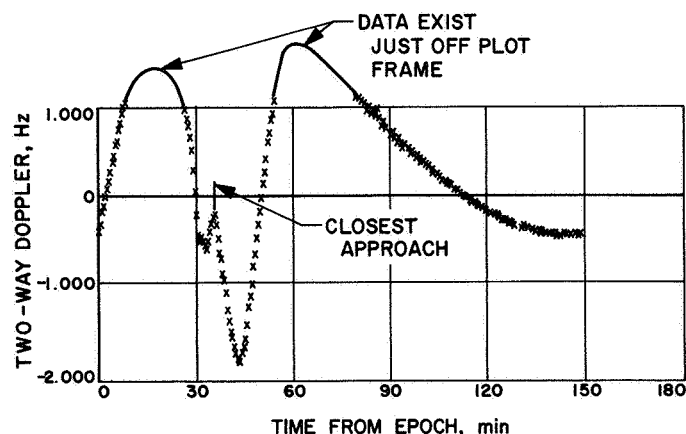


Fig. 15. DSS 41 residuals, Aug. 28, 1966
(12 h 45 min)

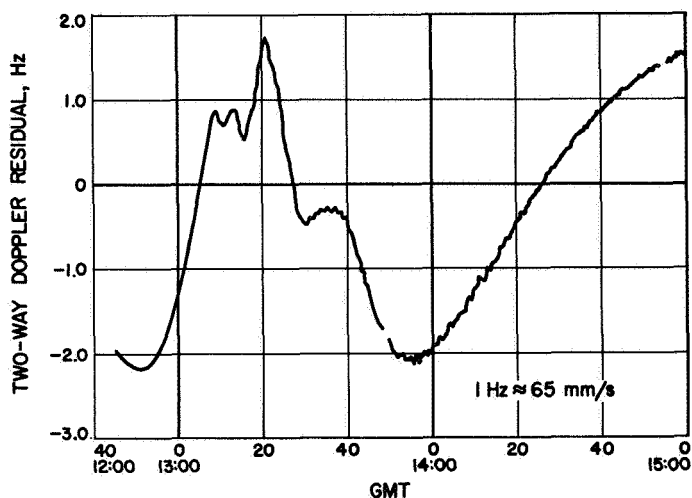


Fig. 16. Doppler residuals, Aug. 28, 1966
(lunar coefficients = 0)

Several orbits of *Lunar Orbiter I* and *II* doppler data were processed through the orbit determination program, where, in some cases, all lunar harmonic coefficients were set to zero, and in others, J20 and C22 were set to nominal values. This essentially removed the effects of the tracking station motion, the point mass gravity, and the earth and sun perturbations from the data, leaving the oblateness perturbations in the residuals. The residuals are illustrated in Figs. 12 through 16. Next, another program converted them to functions of true anomaly for the Fourier transform program. Figures 17 through 21 show the energy density spectrum generated for each orbit. Significantly large amplitudes seem to exist in the frequencies up to 10 Hz. Beyond 10 Hz, the amplitudes appear to be in the noise region.

In Fig. 12, the residuals resulting from fitting a particular orbit in each of two ways are shown, firstly using nominal values of J20 and C22, and secondly for a fit

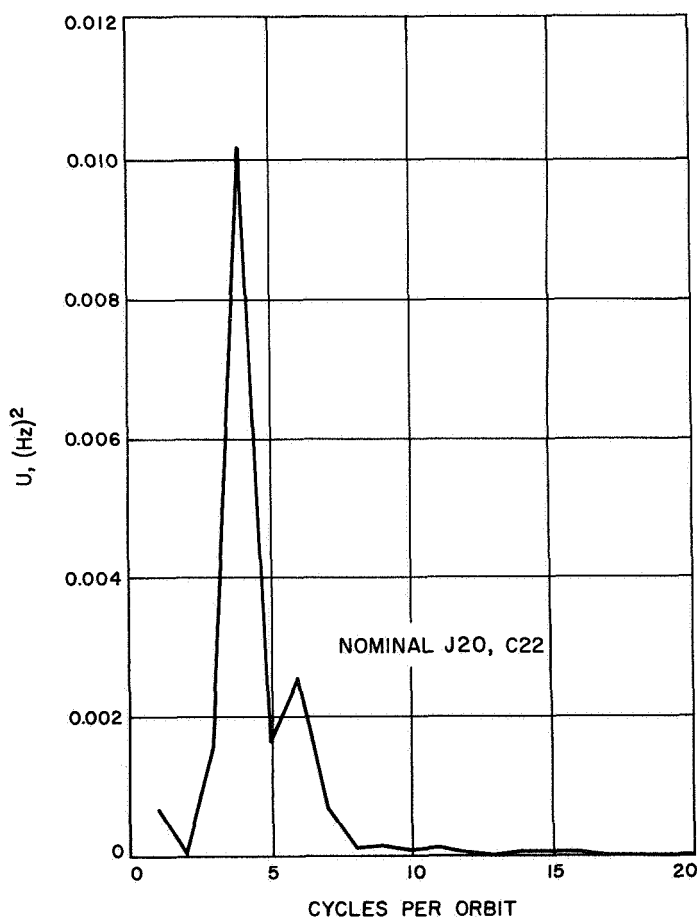


Fig. 17. Energy density, Aug. 26, 1966
(5 h 19 min)

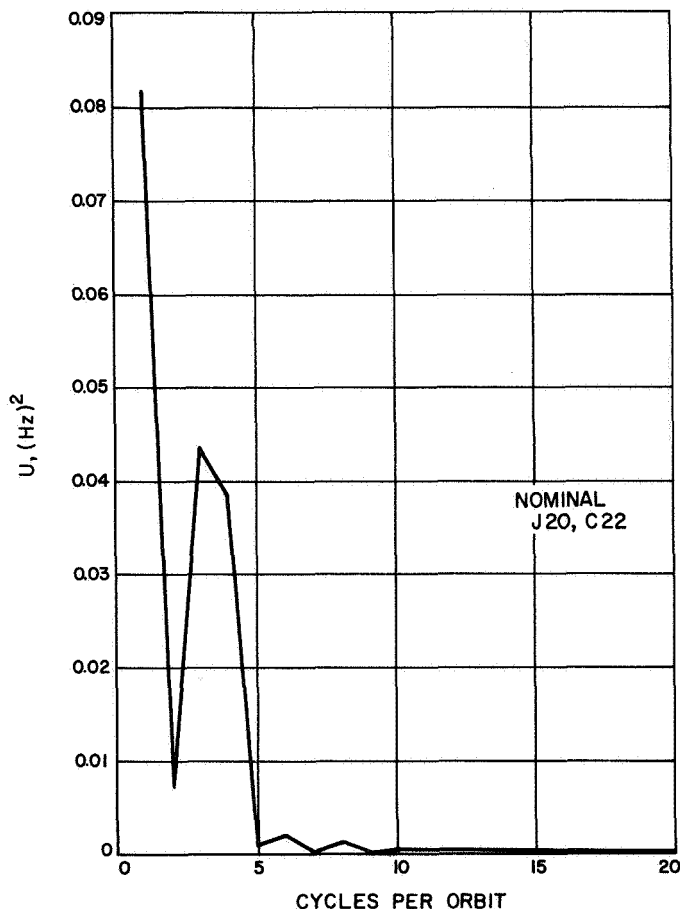
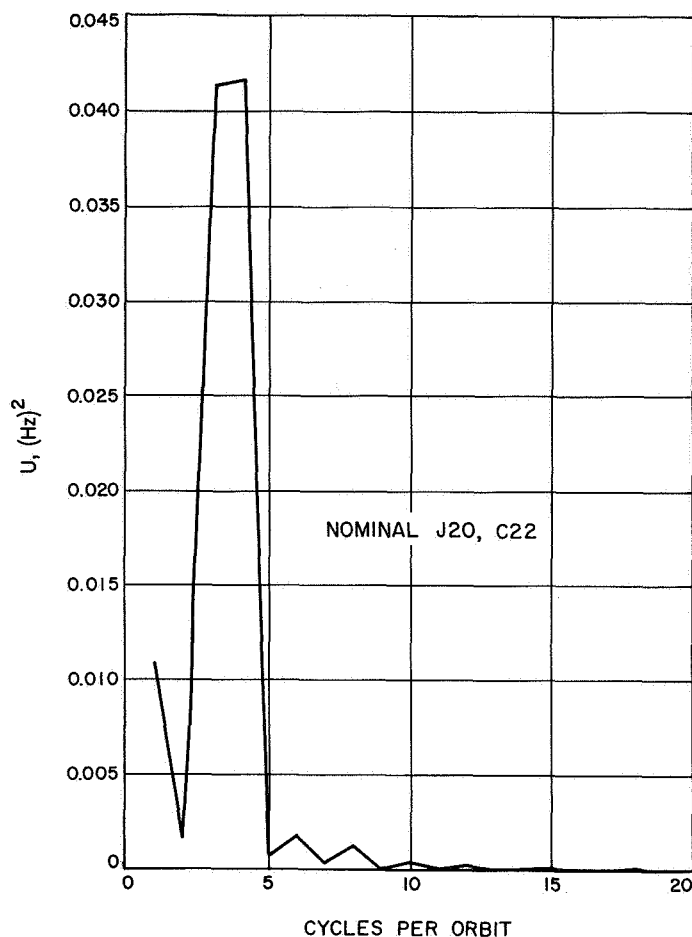


Fig. 18. Energy density, DSS 12, Nov. 22, 1966
(5 h 17 min)



**Fig. 19. Energy density, DSS 41, Nov. 22, 1966
(5 h 17 min)**

where all coefficients are set to zero. Because the signatures are quite similar even with J20 and C22 included, the energy plot is made only for the case with the nominal J20 and C22 included in the fit (Fig. 17). Figures 13 and 14 represent two- and three-way doppler taken at the same time and fit with nominal C22 and J20 coefficients. Again, the signatures are alike. They produce similar energy density plots but there is a difference at 1 Hz per orbit (Figs. 18 and 19). Figures 15 and 16 again represent fits to a particular orbit, but using different gravity models. It is believed their signatures are much different (in contrast to Fig. 12), because this reduction was made on two orbits of data with only one station viewing (i.e., no three-way doppler in the fit as there was in the data for Fig. 12).

For final comparative purposes, however, Figs. 17, 19, and 20 should be studied together, because they represent different orbits using the same nominal J20 and C22 coefficients in the fit. The general patterns exhibited by

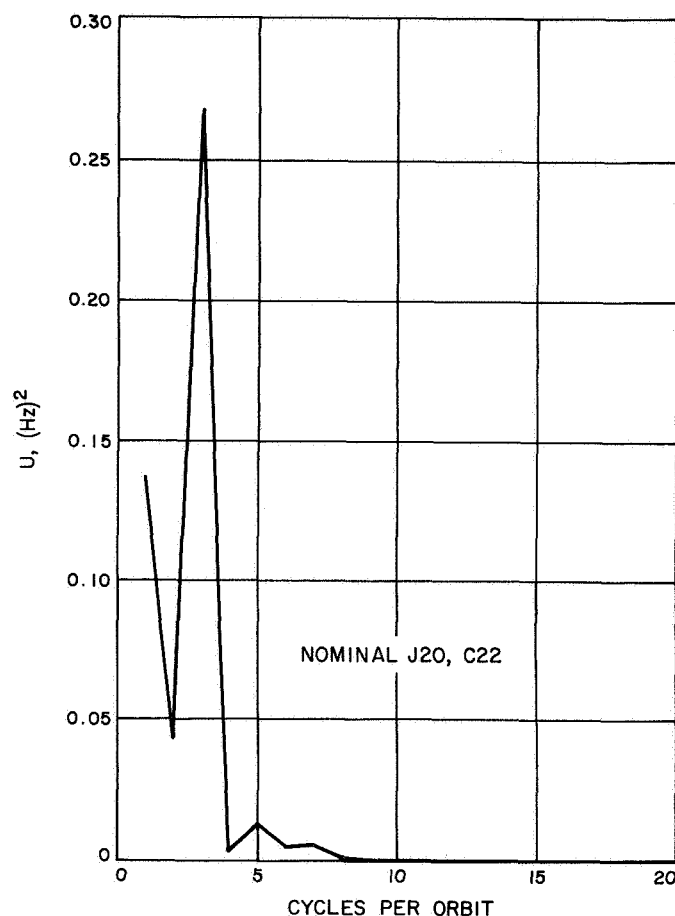


Fig. 20. Energy density, Aug. 28, 1966 (12 h 45 min)

the three figures are similar. However, the detail structure shows many differences. Thus, in Fig. 17, the 4-Hz frequency is dominant, while the 3-Hz frequency has small amplitude. In Fig. 19 the reverse is true. In all three cases, the amplitudes drop to the noise level after 10 Hz. This suggests the inclusion of harmonics up to degree 10 in the potential model.

O. Lunar Ephemeris Position and Velocity Errors Model

Lunar ephemeris errors in position should not cause the doppler residuals. It is shown that position errors of 400 m, which initially cause 20-Hz residuals, are completely removed giving a perfect data fit, good conic element estimates, and show the 400-m discrepancy only in absolute geocentric position.⁶ Velocity errors could be on the order

⁶This is evident in Column 6 of Table 1. Columns 3 and 4 show the effect when ranging data are used in the fit and when the lunar radial scale factor (REM) is not estimated. The orbit is still obtained selenocentrically, but the fit to the data is not as good as when doppler only is used.

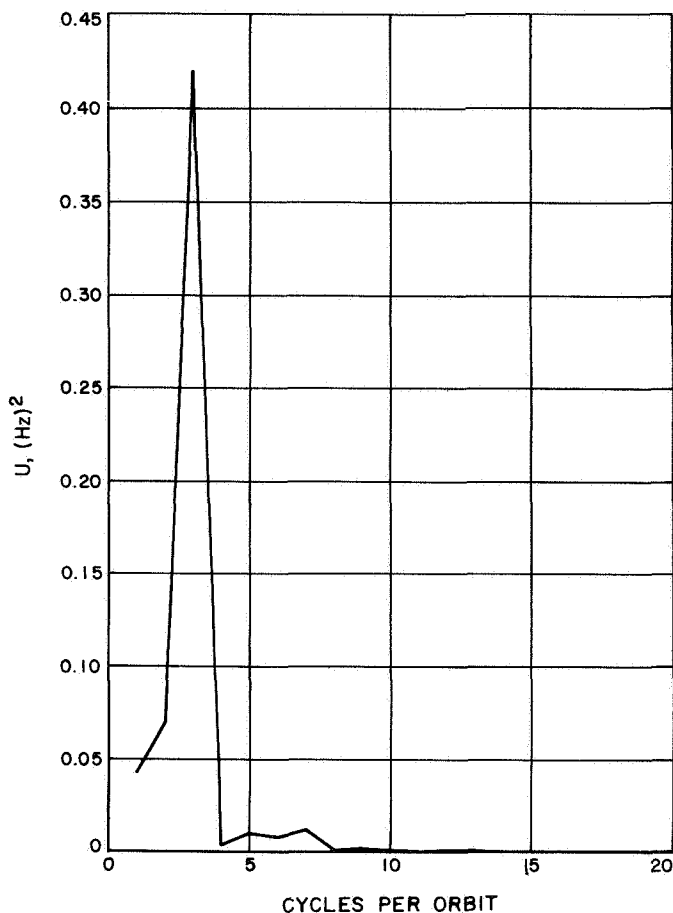


Fig. 21. Energy density, Aug. 28, 1966 (12 h 45 min), lunar coefficients = 0

of Eckert's corrections, which amounted to 1.5 km in 3 days, or a maximum velocity error of 0.05 Hz. This maximum velocity error is small in comparison with the perilune residuals and would frequently be zero. On the other hand, the closest approach residuals are always present. On the basis of these arguments, it is concluded that ephemeris errors are not prime contributors to the perilune residuals.

Another interesting check was effected by simulating 7 h (two orbits) of doppler tracking data with a constant 1-Hz bias to simulate an ephemeris velocity error. The spacecraft position and velocity were then estimated with these corrupted data. Results showed that the bias was not removed and the orbit parameters were changed only slightly.⁷ Figure 22 shows the doppler residuals after the fit. This indicates that a constant velocity error in the computation of the doppler data will surely stand

⁷ $\Delta a = 0.4m$, $\Delta e = 0.000002$, $\Delta i = 0.0006$ deg, $\Delta \Omega = 0.0004$ deg, $\Delta \omega = 0.0004$ deg, $\Delta R = 10m$, $\Delta V = 3$ mm/s.

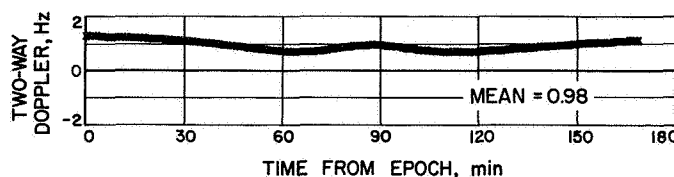


Fig. 22. DSS 41 doppler residuals on bias fit, Aug. 26, 1966 (8 h 20 min)

out and will not significantly degrade solutions. Because in practice constant biases as large as 1 Hz have never been observed in the residuals, ephemeris velocity errors cannot be the source for the pericenter anomalies.

P. Frequency Bias on Three-Way Doppler

Unlike two-way doppler, where the transmitter reference frequency is combined directly with the received frequency, the three-way doppler system (obtained say at Woomera when Goldstone is transmitting and obtaining two-way doppler) uses an atomic clock standard to simulate the transmitter reference frequency. Since the precision of an atomic clock is approximately 1 part in 10^{10} , this may introduce an unknown constant three-way doppler bias as large as ± 0.2 Hz. This bias can be directly estimated in the data processing system. However, whether it is estimated or not, this bias does not significantly change the shape nor the amplitude of the closest approach residuals. This bias seems to be uncorrelated with any of the estimated parameters including the harmonic coefficients and GM.

Q. Radiation Pressure

Although radiation pressure parameters are included in the integration, they do not significantly affect the doppler data over a 7-h period. The acceleration due to solar pressure is approximately 1×10^{-7} m/s². Over an orbit which is completely in the sun, the net effect on energy, and hence on semimajor axis, should be zero. However, even if the accelerations were assumed to act along the orbit in the direction of motion and were integrated over the entire time span of 7 h, the total effect on the doppler would be only 0.04 Hz.

III. Conclusions

Although the results presented herein may not explain the existence of the residuals, they do, however, remove various areas of uncertainty that, at one time or another,

have been considered as reasons for the poor data fit. Therefore, the irregularity of the moon's gravity field (and hence its mass distribution) is more conclusively

established. This irregularity is exhibited by gravity harmonics of high degree (eight and above), which contribute measurably to the spacecraft accelerations.

Table 1. Perturbations caused by lunar ephemeris errors

Coordinate System	Parameters	Δ Longitude ≈ 200 m Do not estimate REM	Δ REM ≈ 400 m Do not estimate REM	Δ Longitude ≈ 200 m Δ REM ≈ 400 m Estimate REM	Δ REM ≈ 400 m No range pt. Do not estimate REM	1 σ Uncertainty
Selenocentric	ΔX , m	1.0	12.	0.2	0.0001	21.
	ΔY , m	0.5	12.	1.	0.0002	114.
	ΔZ , m	2.0	9.	1.	0.0030	202.
	$\Delta \dot{X}$, m/s	0.0008	0.026	0.001	0.0002	0.016
	$\Delta \dot{Y}$, m/s	0.0024	0.11	0.005	0.0003	0.065
	$\Delta \dot{Z}$, m/s	0.0021	0.18	0.007	0.0004	0.089
Geocentric	ΔX , m	90.	-328.	98.	-343.	
	ΔY , m	-166.	-226.	-158.	-166.	
	ΔZ , m	-94.	64.	-97.	-54.	
	$\Delta \dot{X}$, m/s	0.0007	0.018	0.00009	0.0005	
	$\Delta \dot{Y}$, m/s	0.0015	-0.065	0.0035	-0.001	
	$\Delta \dot{Z}$, m/s	-0.0003	0.088	-0.0031	-0.0003	
	Δ REM			6.71		
Selenocentric conic	Δa , m	0.1	0.6	0.5	0.00000	
	Δe	0.00000003	0.0000021	0.00000008	0.00000002	
	Δi deg	0.000084	0.007	0.00019	0.00002	
	$\Delta \Omega$ deg	0.00019	0.004	0.00028	0.00001	
	$\Delta \omega$ deg	0.00024	0.004	0.00030	0.000006	
	$\Delta \nu$ deg	0.00000007	0.000003	0.00000003	0.000001	
	Maximum residual					
	Before convergence	D ^a 10. Hz R ^a 168 m	D 20. Hz R 35 m	D 30. Hz R 144 m	D 20. Hz	
	After convergence	D 0.004 Hz R 12 m	D 0.06 Hz R 375 m	D 0.03 Hz R 4 m	D 0.001 Hz	

^aD = Doppler, R = Ranging.

References

1. Lorell, J., Sjogren, W. L., and Boggs, D., *Compressed Tracking Data Used for First Iteration in Selenodesy Experiment, Lunar Orbiters I and II*, Technical Memorandum 33-343, Jet Propulsion Laboratory, Pasadena, California, May 1, 1967.
2. Liu, A., *Results of the Doppler-Ranging Calibration Experiment—Phase I, II, Experiment I*, SPS 37-46, Vol. III, Jet Propulsion Laboratory, Pasadena, California, June 23, 1967, pp. 23-28.